

Are your **MRI contrast agents** cost-effective?

Learn more about generic **Gadolinium-Based Contrast Agents**.



FRESENIUS  
KABI

caring for life

# AJNR

This information is current as  
of April 17, 2024.

## **MR Imaging of the Enlarged Endolymphatic Duct and Sac Syndrome by Use of a 3D Fast Asymmetric Spin-echo Sequence: Volume and Signal-intensity Measurement of the Endolymphatic Duct and Sac and Area Measurement of the Cochlear Modiolus**

Shinji Naganawa, Tokiko Koshikawa, Eriko Iwayama, Hiroshi Fukatsu, Tsuneo Ishiguchi, Takeo Ishigaki, Mitsuru Ikeda, Tsutomu Nakashima and Nobuyasu Ichinose

*AJNR Am J Neuroradiol* 2000, 21 (9) 1664-1669

<http://www.ajnr.org/content/21/9/1664>

# MR Imaging of the Enlarged Endolymphatic Duct and Sac Syndrome by Use of a 3D Fast Asymmetric Spin-echo Sequence: Volume and Signal-intensity Measurement of the Endolymphatic Duct and Sac and Area Measurement of the Cochlear Modiolus

Shinji Naganawa, Tokiko Koshikawa, Eriko Iwayama, Hiroshi Fukatsu, Tsuneo Ishiguchi, Takeo Ishigaki, Mitsuru Ikeda, Tsutomu Nakashima, and Nobuyasu Ichinose

**BACKGROUND AND PURPOSE:** In enlarged endolymphatic duct (EED) and sac (EES) syndrome, deformity of the EED and EES is congenital; however, hearing loss is acquired. To investigate the pathophysiology of progressive sensorineural hearing loss in EED and EES syndrome, we measured the volume of the EED and EES, the diameter of the EED and EES, the area of the cochlear modiolus, and the signal intensity of the EES and compared our findings against degree of hearing loss.

**METHODS:** Thin-section MR images of 33 ears in 17 patients with EED and EES syndrome were studied. All studies were obtained on a 1.5-T MR unit using a quadrature surface phased-array coil. Heavily T2-weighted 3D fast asymmetric spin-echo images were obtained with a voxel size of  $0.3 \times 0.3 \times 0.8$  mm without zero-fill interpolation. Two radiologists traced the areas of the EED and EES manually, and the volume was calculated. The area of the cochlear modiolus, diameter of the EED and EES, and signal intensity of the EES were also measured by drawing regions of interest manually. The signal intensity ratio of EES/CSF was calculated. These measured values were compared against audiographic data, and the degree of linear correlation was determined.

**RESULTS:** The volume of the EED and EES, the area of the modiolus, the diameter of the EED and EES, and the signal intensity of the EES did not show significant correlation with degree of hearing loss.

**CONCLUSION:** These findings suggest that there is a microscopic area of damage or fragility in the inner ear not visible even with thin-section heavily T2-weighted MR imaging.

Large vestibular aqueduct syndrome, or enlarged endolymphatic duct (EED) and sac (EES) syndrome, is an inner ear malformation that manifests as progressive sensorineural hearing loss starting in infancy or childhood (1–3). The deformity of the EED and EES is congenital (4); however, hearing loss in this syndrome is acquired (4, 5). A distinct

feature is that hearing loss in EED and EES syndrome is triggered by minor head trauma (3). Although the true pathogenesis of the hearing loss in this syndrome is still unknown, several theories as to its pathophysiology have been proposed (5–11). In one recent CT study (9), all ears with a large vestibular aqueduct had associated cochlear modiolus deficiencies. On the basis of this finding, the authors suggested the theory that progressive hearing loss in the presence of a large vestibular aqueduct is caused by the transmission of subarachnoid pressure forces in the internal auditory canal into the labyrinth through a deficient cochlear modiolus, resulting in damage to the hair cells. On the other hand, a recent MR study reported that the presence of a large EED and EES was frequently associated with cochlear modiolus deficiencies, but that some patients had a normal modiolus, even when hearing loss developed (12). The findings of

Received December 17, 1999; accepted after revision March 22, 2000.

From the Departments of Radiology (S.N., T.K., E.I., H.F., Ts.I., Ta.I), Medical Information and Records (M.I.), and Otolaryngology (T.N.), Nagoya University School of Medicine, Nagoya, Japan; and Toshiba Nasu Works, Tochigi, Japan (N.I.).

Address reprint requests to Shinji Naganawa, MD, Department of Radiology, Nagoya University School of Medicine, 65 Tsurumai-cho, Showa-ku, Nagoya 466-8550, Japan.

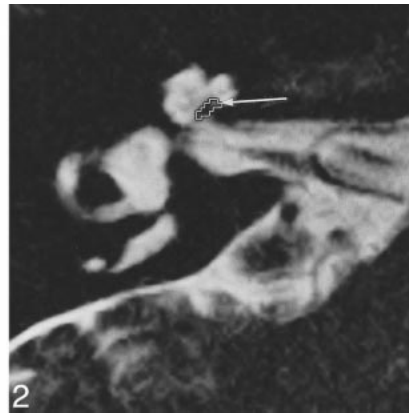
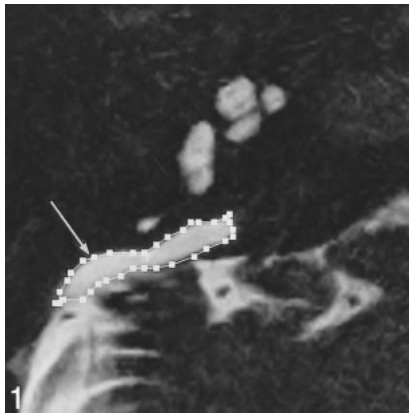


FIG 1. Axial T2-weighted fast spin-echo image (4000/240/1; 0.8-mm thick) in an 18-year-old woman with EED and EES syndrome. The area of the EES is outlined (arrow).

FIG 2. Axial T2-weighted fast spin-echo image (4000/240/1; 0.8-mm thick) in a 20-year-old man with EED and EES syndrome. The area of the cochlear modioli is outlined (arrow).

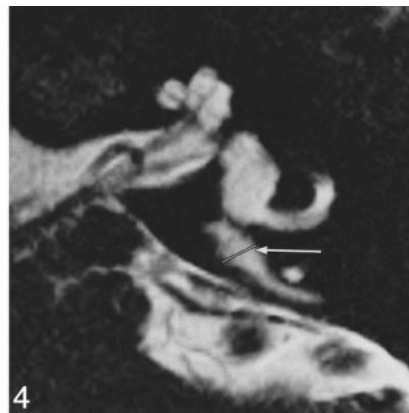


FIG 3. Axial heavily T2-weighted image (4000/240/1; 0.8-mm thick) in a 19-year-old man with EED and EES syndrome. A septumlike structure (arrow) is seen in the intraosseous EES. The signal of the posterior, dural portion of the EES (arrowheads) is lower than that of the intraosseous portion.

FIG 4. Axial T2-weighted fast spin-echo image (4000/240/1; 0.8-mm thick) in a 20-year-old man with EED and EES syndrome. The diameter of the EED and EES is indicated with a white line (arrow) at the midpoint between the common crus and its external aperture. In this case, the diameter is 2.4 mm.

this MR study do not necessarily support the previously suggested pressure wave theory. Rather, they support another previously suggested theory that hyperosmolar proteins in the EES reflux into the cochlear duct through a widely patent EED, causing osmotic damage to the neuroepithelium (6–8, 13). Another recent CT study reported that the degree of modiolar deficiency did not consistently correspond to the severity of hearing loss, although the morphology and thickness of the vestibular aqueduct did correlate strongly with the degree of hearing loss (14). Still another study reported that the diameter of the EED did not correspond to the degree of hearing loss (2). To clarify these controversial points, we investigated the relationship between severity of hearing loss, as determined by air-conduction audiographic data, and EED and EES volume, area of the cochlear modioli, and signal intensity of the EES, as determined by 3D Fourier transformation thin-section MR imaging.

### Methods

All studies were performed on a 1.5-T MR system using a quadrature surface phased-array coil. A pair of these quadrature surface coils was used as a phased array, with one coil placed over each ear. The heavily T2-weighted 3D fast asymmetric spin-echo pulse sequence was obtained with the following parameters: TR/TE/excitations = 4000/240/1, echo train length = 79, field of view = 16 cm, slice thickness = 0.8 mm, axial slab matrix =  $512 \times 512 \times 40$ , voxel size =  $0.3$

$\times 0.3 \times 0.8$  mm without zero-fill interpolation, and scan time = 11 minutes 48 seconds. This equipment and pulse sequence have been described in detail earlier (12, 15, 16).

Thin-section MR images were obtained in 33 ears in 17 patients with EED and EES syndrome (one patient had unilateral disease). Seven patients were male and 10 were female; ages ranged from 4 to 33 years (mean age  $\pm$  SD,  $15.0 \pm 9.4$  years). The EED and EES are considered to be dilated when the diameter at the midpoint between the common crus and its external aperture is 1.5 mm or more on thin-section MR images (17). Two radiologists traced the area of the EED and EES as a single area manually on the MR console for each slice, and the volumes were obtained by summing each measured area multiplied by the slice thickness (Fig 1). The area of the cochlear modioli and the signal intensity of the EES were also measured by drawing regions of interest manually. The area of the cochlear modioli was measured in the axial slice in which the cochlear modioli was visualized at its maximum size on thin-section T2-weighted images (Fig 2). The signal intensity ratio of the EES relative to that of adjacent CSF was calculated. The region of interest was drawn as large as possible in the EES. When the EES showed nonuniform signal, the signal intensity measurements were obtained from a region of interest drawn in the area of lower signal intensity (Fig 3). The signal intensity of adjacent CSF was measured by drawing a region of interest in the internal auditory canal, where the distance from the surface coil is similar to that of the EES and pulsatile motion of the CSF is relatively small (18). For modiolar area measurements, the area of low signal intensity with a distinctly triangular or trapezoidal shape at the axis of the basal turn or the basal and middle turn of the cochlea was outlined, excluding the free, thin part of the osseous spiral lamina and interscalar septum (9, 12). The diameter of the EED and EES was measured at the midpoint between the common crus and its external aperture (Fig 4). At the console,

**TABLE 1: Summary of patient data and results of the measurements**

Patient No.	Age (y)/ Sex	Vertigo	R/L	Average Hearing Level (dB)	Area of Cochlear Modiolus (mm <sup>2</sup> ) (Observer 1, 2)	Volume of EES and EED (mm <sup>3</sup> ) (Observer 1, 2)	Signal Intensity Ratio of EES/CSF (Observer 1, 2)	Diameter of EED and EES (mm) (Observer 1, 2)
1	19/M	( + )	R	96.7	1.98 (1.97, 1.96)	488.0 (476, 500)	0.61 (0.62, 0.60)	2.0 (2.0, 2.0)
			L	100	1.81 (1.70, 1.92)	485.8 (475, 495.8)	0.59 (0.58, 0.60)	3.1 (3.1, 3.1)
2	27/M	( + )	R	103.3	5.17 (5.12, 5.22)	95.5 (89.5, 101.5)	1.04 (1.04, 1.04)	1.6 (1.5, 1.7)
			L	30	4.30 (4.12, 4.48)	246.0 (237, 255)	0.72 (0.73, 0.71)	2.0 (2.0, 2.0)
3	20/F	( - )	R	76.7	1.27 (1.33, 1.21)	686.9 (681.4, 692.4)	1.10 (1.08, 1.12)	2.7 (2.7, 2.7)
			L	108.3	0.98 (0.99, 0.97)	687.9 (653.5, 722.3)	1.08 (1.06, 1.10)	3.2 (3.1, 3.3)
4	18/F	( - )	R	80	1.86 (1.85, 1.87)	533.8 (512.4, 555.2)	0.89 (0.88, 0.90)	3.8 (3.8, 3.8)
			L	80	1.56 (1.52, 1.60)	655.9 (649.3, 662.5)	0.07 (0.07, 0.07)	3.1 (3.0, 3.2)
5	4/M	( - )	R	53.3	1.56 (1.58, 1.54)	370.5 (377.9, 363.1)	1.07 (1.05, 1.09)	2.8 (2.6, 2.9)
			L	63.3	1.86 (1.82, 1.90)	216.5 (223.0, 210.0)	1.35 (1.34, 1.36)	2.4 (2.5, 2.3)
6	33/F	( - )	R	103.3	4.00 (4.22, 3.78)	500.6 (465.8, 535.4)	0.34 (0.32, 0.36)	1.8 (1.8, 1.8)
			L	86.7	4.00 (4.10, 3.90)	361.8 (359.5, 364.1)	0.65 (0.68, 0.62)	2.3 (2.2, 2.4)
7	14/F	( - )	R	48.3	1.67 (1.6, 1.74)	554.1 (549.5, 558.7)	0.85 (0.80, 0.90)	2.8 (2.7, 2.9)
			L	110	1.86 (1.89, 1.83)	478.0 (481.2, 474.8)	0.84 (0.88, 0.80)	2.9 (2.9, 2.9)
8	22/F	( + )	R	110	1.46 (1.39, 1.53)	143 (146.6, 139.4)	0.38 (0.37, 0.39)	3.0 (3.0, 3.0)
			L	100	1.46 (1.44, 1.48)	302.7 (299.7, 305.7)	0.74 (0.71, 0.77)	2.1 (2.0, 2.2)
9	4/M	( - )	R	86.7	4.00 (3.80, 4.20)	480.0 (475.2, 484.8)	0.80 (0.76, 0.84)	2.2 (2.3, 2.1)
			L	90	4.00 (4.00, 4.00)	500 (518.2, 481.8)	0.80 (0.81, 0.79)	2.3 (2.3, 2.3)
10	6/F	( - )	R	86.7	4.00 (3.88, 4.12)	383.8 (368.5, 399.2)	0.39 (0.35, 0.43)	3.1 (3.0, 3.2)
			L	46.7	1.37 (1.32, 1.42)	318.1 (308.6, 327.6)	0.83 (0.81, 0.85)	3.6 (3.7, 3.5)
11	5/F	( - )	R	63.3	1.95 (1.91, 1.99)	709.0 (676.8, 741.2)	1.01 (1.00, 1.02)	3.5 (3.5, 3.5)
			L	110	1.46 (1.49, 1.43)	358.6 (376.5, 340.7)	1.09 (1.05, 1.13)	1.6 (1.5, 1.7)
12	31/F	( + )	R	8.3	5.86 (5.66, 6.26)	58.1 (57.8, 58.4)	0.58 (0.56, 0.60)	2.3 (2.3, 2.3)
			L	60	1.95 (1.99, 1.91)	55.5 (53.3, 57.7)	0.65 (0.62, 0.68)	2.0 (2.1, 1.9)
13	10/F	( + )	R	103.3	3.22 (3.25, 3.19)	419.2 (402.4, 436.0)	0.65 (0.64, 0.66)	2.5 (2.4, 2.6)
			L	85	1.27 (1.30, 1.24)	406.0 (382.7, 429.3)	0.74 (0.76, 0.72)	2.7 (2.8, 2.6)
14	20/M	( - )	R	90	1.96 (2.00, 1.92)	207.2 (211.3, 203.1)	0.76 (0.76, 0.76)	2.7 (2.8, 2.5)
			L	90	1.86 (1.92, 1.80)	412.6 (408.5, 416.7)	1.14 (1.11, 1.17)	3.3 (3.4, 3.2)
15	6/M	( - )	R	85	1.08 (1.02, 1.14)	199.2 (205.2, 193.2)	0.92 (0.95, 0.89)	2.6 (2.5, 2.7)
			L	82.5	1.96 (1.99, 1.93)	524.4 (524.7, 524.1)	1.19 (1.15, 1.23)	3.4 (3.4, 3.4)
16	8/M	( - )	R	76.7	4.51 (4.21, 4.81)	120.0 (118.0, 122.0)	0.84 (0.83, 0.85)	3.3 (3.2, 3.4)
			L	62.7	1.47 (1.41, 1.53)	260.4 (258.0, 262.8)	0.48 (0.46, 0.50)	3.2 (3.1, 3.3)
17	20/F	( - )	R	95	4.00 (3.78, 4.22)	102.2 (95.2, 107.2)	1.24 (1.24, 1.24)	1.6 (1.6, 1.6)
Mean	15			80.5	2.46	381.8	0.79	2.68
SD	9.4			24	1.33	182.7	0.28	0.58

**TABLE 2: Correlation coefficient (r), r<sup>2</sup>, and P value**

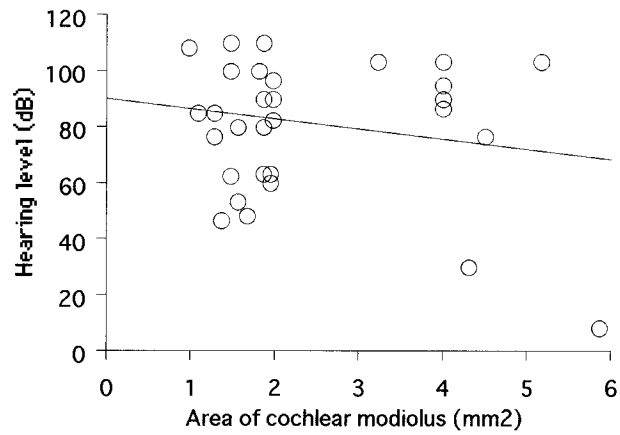
	Correlation Coefficient (r)	r <sup>2</sup>	P Value (two tail)
Area of cochlear modiolus (mm <sup>2</sup> )	-0.2	0.040000	.266
Volume of EES and EED (mm <sup>3</sup> )	0.216	0.046656	.227
Signal intensity ratio of EES/CSF	-0.001	0.000001	.997
Diameter of EED and EES (mm)	-0.133	0.017689	.461
Age	-0.018	0.000324	.921

the window width was set to 100% of the range from the lowest to the highest pixel values in the image, and the window center level was set to the midpoint between the lowest and highest pixel values. Each radiologist performed each measurement twice, and the average of the two measurements was obtained. The final value was established by averaging the values obtained by the two observers. Interobserver and intraobserver variability were also assessed.

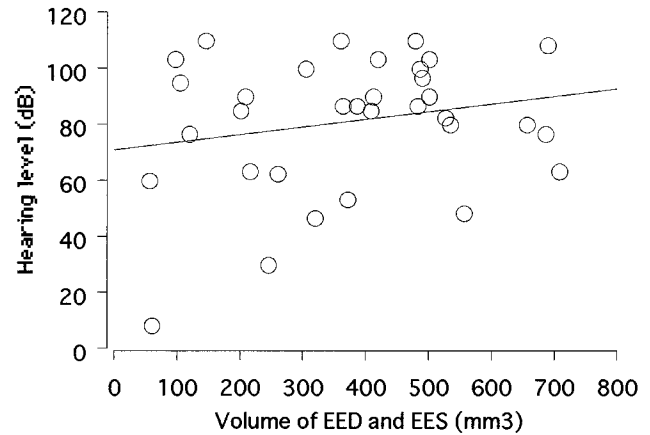
All patients were examined during the period from April 1996 to April 1999. The study protocol was approved by our institutional medical ethics committee, and informed consent to participate in the study was obtained from all patients or their legal guardians.

**TABLE 3: r<sup>2</sup> values at each frequency**

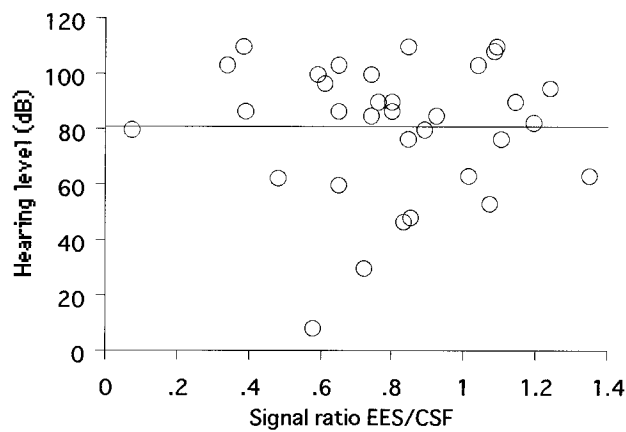
	250 Hz	500 Hz	1000 Hz	2000 Hz	4000 Hz
Area of cochlear modiolus (mm <sup>2</sup> )	0.0441	0.0256	0.0484	0.0529	0.0441
Volume of EES and EED (mm <sup>3</sup> )	0.0225	0.0225	0.0441	0.0841	0.1156
Signal intensity ratio of EES/CSF	0.000256	0.0016	0.0025	0.0025	0.0144
Diameter of EED and EES (mm)	0.0016	0.0025	0.0196	0.0256	0.0196
Age	0.0289	0.0225	0.0001	0.0064	0.0121



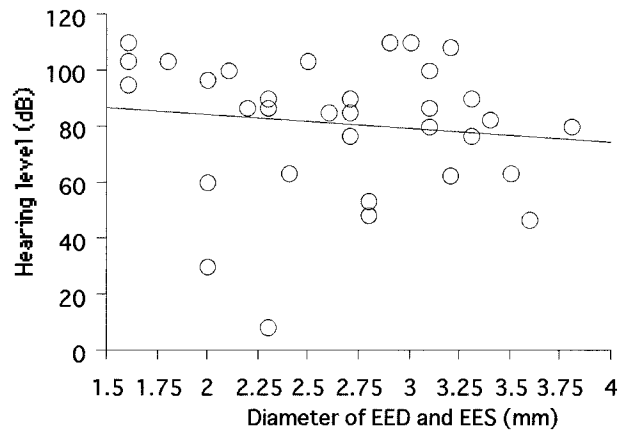
**A**  $Y = 89.878 - 3.556 * X; R^2 = .04$



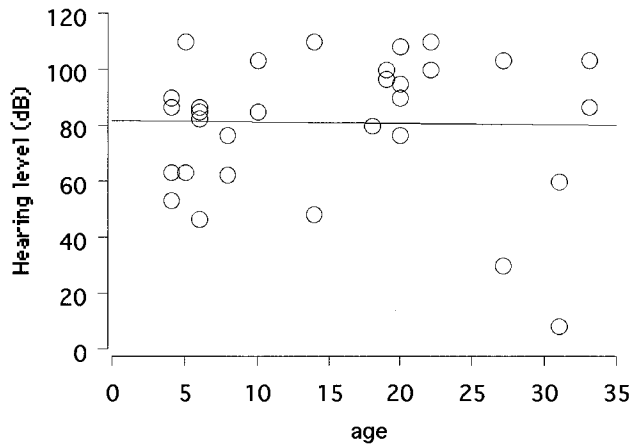
**B**  $Y = 70.658 + .028 * X; R^2 = .047$



**C**  $Y = 81.016 - .066 * X; R^2 = 6.116E-7$



**D**  $Y = 94.805 - 5.22 * X; R^2 = .018$



**E**  $Y = 81.681 - .046 * X; R^2 = 3.265E-4$

FIG 5. A-E, Scatter plots of the average hearing level versus area of the cochlear modiolus (A), volume of the EED and EES (B), signal intensity ratio of EES/CSF (C), diameter of the EED and EES (D), and patient age (E). None of these values correlated with hearing level.

All ears showed progressive sensorineural hearing loss. The average hearing level was determined on the basis of the average of the air-conduction audiographic data obtained at 500, 1000, and 2000 Hz. Audiograms were obtained within 1 month of the MR examinations. These measured values and the patients' ages were compared against audiographic data at each frequency (250, 500, 1000, 2000, 4000 Hz) and against the average hearing level. The linear correlation was determined by simple regression analysis.

### Results

Patient data and results of each observer's measurements are summarized in Table 1. No significant correlation was found between volume of the EED and EES, area of the modiolus, signal intensity of the EES, diameter of the EED and EES, or patient age and the degree of hearing loss at any

frequency and average hearing level. The correlation coefficients are listed in Tables 2 and 3. Scatter plots of the average hearing level versus each value are shown in Figure 5. Intraobserver variability for both observers and interobserver variability were less than 15% for all measurements.

### Discussion

The volumetric measurement of inner ear fluid has been reported by Melhem et al (19). These authors used 3D T2-weighted fast spin-echo images for measuring total labyrinthine fluid and obtained reproducible results using a voxel size of  $0.6 \times 0.6 \times 0.6$  mm. In the present study, a voxel size of  $0.3 \times 0.3 \times 0.8$  mm was used, and showed relatively small intraobserver and interobserver variability. We therefore believe that the values obtained in the present study are reliable.

According to the findings of a previous study using CT, a deficient modiolus is said to allow the transmission of CSF pressure waves into the labyrinth, resulting in damage to the hair cells in the organ of Corti (9). A recent MR study confirmed that a large EED and EES were frequently associated with modiolar deficiency but that some patients had a normal modiolar area (12). One recent CT study reported that the degree of modiolar deficiency did not consistently correspond to the severity of hearing loss; however, the morphology and thickness of the vestibular aqueduct were strongly correlated with the degree of hearing loss (14). The results of the present study also showed that the degree of cochlear deficiency did not correspond to hearing level, suggesting the possibility that a microscopic area of damage or fragility in the inner ear is not seen even on high-resolution MR images.

Another theory suggests that hyperosmolar proteins in the enlarged EES reflux into the ductus cochlearis (scala media) through a widely patent EED, causing osmotic damage to the neuroepithelium (6–8, 13, 20). It has been reported that the protein concentration in the EES is quite high (1000–3000 mg/dL) even in healthy subjects (8). In one patient with EED and EES syndrome, the protein concentration in the EES was reported to be 660 mg/dL (21). However, the signal intensity of the EES varied from patient to patient, suggesting that the protein concentration also varies from patient to patient (22). The signal intensity of the EES was reported to be higher than that of CSF on T1-weighted images and lower on T2-weighted images in eight of 10 ears in patients with EED and EES syndrome, suggesting a high protein content within the EES (7, 8). In the present study, the signal intensity values of the EES did not correspond to hearing level. The results of the present study do not directly support the latter theory. Signal intensity on T2-weighted images of the EES may differ from that at the time the insult to the neuroepithelium occurred. The fluid with high pro-

tein concentration shows lower signal intensity on heavily T2-weighted images (23). However, sludge or extravasated blood also can cause the signal reduction. Thus, signal intensity may not directly correlate with protein concentration.

In the present study, only five of 17 patients experienced vertigo during the follow-up period. The EED is connected with the labyrinth at the vestibule, and symptoms of vestibular disturbance would be expected to appear if pressure waves or hyperosmolar fluid reflux through the EED were responsible for the hearing loss.

EED and EES syndrome has a genetic component (22, 24), and patients with this syndrome have simply been advised to avoid contact sports. Recently, however, the use of cochlear implants in patients with EES and EED syndrome has been advocated, although there is the risk of a perilymph gusher (25). EES and EED syndrome is sometimes associated with fixation of the stapes or abnormality of the round window, resulting in stapes gusher or perilymph fistula (26–28). High-resolution MR imaging is useful as a presurgical examination to evaluate cochlear patency in cochlear implant candidates (29).

### Conclusion

The modiolar area and volume of the EED and EES do not correlate with the severity of hearing loss. These results suggest that there is a microscopic area of damage or fragility in the inner ear not visible even with current high-resolution T2-weighted MR imaging.

### References

1. Mafee MF, Charlette D, Kumar A, Belmont H. **Large vestibular aqueduct and congenital sensorineural hearing loss.** *AJNR Am J Neuroradiol* 1992;13:805–819
2. Dahlen RT, Harnsberger HR, Gray SD, et al. **Overlapping thin section fast spin echo MR of the large vestibular aqueduct syndrome: comparison with CT.** *AJNR Am J Neuroradiol* 1997;18:67–75
3. Okumura T, Takahashi H, Honjo I, Takagi A, Mitamura K. **Sensorineural hearing loss in patients with large vestibular aqueduct.** *Laryngoscope* 1995;105:289–294
4. Emmett JR. **The large vestibular aqueduct syndrome.** *Am J Otol* 1985;6:387–415
5. Valvassori GE, Clemis JD. **The large vestibular aqueduct syndrome.** *Laryngoscope* 1978;88:723–728
6. Wilson DF, Hodgson RS, Talbot JM. **Endolymphatic sac obliteration for large vestibular aqueduct syndrome.** *Am J Otol* 1997;1:101–107
7. Okamoto K, Ito J, Furusawa T, Sakai K, Tokiguchi S. **Large vestibular aqueduct syndrome with high CT density and high MR signal intensity.** *AJNR Am J Neuroradiol* 1997;18:482–484
8. Okamoto K, Ito J, Furusawa T, Sakai K, Horikawa S, Tokiguchi S. **MRI of enlarged endolymphatic sacs in the large vestibular aqueduct syndrome.** *Neuroradiology* 1998;40:167–172
9. Lemmerling MM, Mancuso AA, Antonelli PJ, Kubilis PS. **Normal modiolus: CT appearance in patients with a large vestibular aqueduct.** *Radiology* 1997;204:213–219
10. Okumura T, Takahashi H, Honjo I, et al. **Vestibular function in patients with a large vestibular aqueduct.** *Acta Otolaryngol Suppl (Stockh)* 1995;520:323–326
11. Okumura T, Takahashi H, Honjo I, Takagi A, Azato R. **Magnetic resonance imaging of patients with large vestibular aqueducts.** *Eur Arch Otorhinolaryngol* 1996;253:425–428

12. Naganawa S, Ito T, Iwayama E, et al. **MR imaging of the cochlear modiolus: area measurement in normal subjects and in patients with a large endolymphatic duct and sac.** *Radiology* 1999;231:819–823
13. Levenson MJ, Parisier SC, Jacobs M, Edelstein DR. **The large vestibular aqueduct syndrome in children: a review of 12 cases and the description of a new clinical entity.** *Arch Otolaryngol Head Neck Surg* 1989;115:54–58
14. Antonelli PJ, Nall AV, Lemmerling MM, Mancuso AA, Kubilis PS. **Hearing loss with cochlear modiolar defects and large vestibular aqueducts.** *Am J Otol* 1998;19:306–312
15. Naganawa S, Ito T, Fukatsu H, et al. **Three-dimensional fast spin echo MR of the inner ear: ultra-long ETL and half-Fourier technique.** *AJNR Am J Neuroradiol* 1998;19:739–741
16. Naganawa S, Ito T, Fukatsu H, et al. **MR imaging of the inner ear: comparison of a three-dimensional fast spin-echo sequence with use of a dedicated quadrature-surface phased array coil with a gadolinium-enhanced spoiled gradient recalled sequence.** *Radiology* 1998;208:679–685
17. Harnsberger HR, Dahlen RT, Shelton C, Gray SD, Parkin JL. **Advanced techniques in magnetic resonance imaging in the evaluation of the large endolymphatic duct and sac syndrome.** *Laryngoscope* 1995;105:1037–1042
18. Iwayama E, Naganawa S, Ito T, et al. **High-resolution MR cisternography of the cerebellopontine angle: 2D versus 3D fast spin-echo sequences.** *AJNR Am J Neuroradiol* 1999;20:889–895
19. Melhem ER, Shakir H, Bakthavachalam S, et al. **Inner ear volumetric measurements using high-resolution 3D T2-weighted fast spin-echo MR imaging: initial experience in healthy subjects.** *AJNR Am J Neuroradiol* 1998;19:1819–1822
20. Hirsch BE, Weissman JL, Curtin HD, Kamerer DB. **Magnetic resonance imaging of the large vestibular aqueduct.** *Arch Otolaryngol Head Neck Surg* 1992;118:1124–1127
21. Jackler RK, Cruz ADL. **The large vestibular aqueduct syndrome.** *Laryngoscope* 1989;99:1238–1243
22. Phelps PD, Coffey RA, Trembath RC, et al. **Radiological malformations of the ear in Pendred syndrome.** *Clin Radiol* 1998;53:268–273
23. Sai J, Ariyama J. **MRCF: Early Diagnosis of Pancreatobiliary Disease: T2-Shortening Bile.** Tokyo: Springer;2000;66–67
24. Tong KA, Harnsberger HR, Dahlen RT, Carey JC, Ward K. **Large vestibular aqueduct syndrome: a genetic disease?** *AJR Am J Roentgenol* 1997;168:1097–1101
25. Aschendorff A, Marangos N, Laszig R. **Large vestibular aqueduct syndrome and its implication for cochlear implant surgery.** *Am J Otol* 1997;18 (Suppl):S57
26. Schessel DA, Nedzelski JM. **Presentation of large vestibular aqueduct syndrome to a dizziness unit.** *J Otolaryngol* 1992;21:265–269
27. Belenky WA, Madgy DN, Leider JS, Becker CJ, Hotaling AJ. **The enlarged vestibular aqueduct syndrome (EVA syndrome).** *Ear Nose Throat J* 1993;72:746–751
28. Shirazi A, Fenton JE, Fagan PA. **Large vestibular aqueduct syndrome and stapes fixation.** *J Laryngol Otol* 1994;108:989–990
29. Ito T, Naganawa S, Fukatsu H, et al. **High resolution MR images of the inner ear internal anatomy using a local gradient coil at 1.5 tesla: Correlation with histological specimen.** *Radiat Med* 1999;17:343–347